Temporal Variations of the Indoor Wireless Millimeter-Wave Channel

Paul Marinier, Gilles Y. Delisle, *Senior Member, IEEE*, and Charles L. Despins

***Abstract*—This paper reports experiments conducted near 30 GHz to characterize human-induced variations of an indoor radio channel for which both terminals are stationary. The dependence of envelope characteristics on various parameters (degree and localization of movement, terminal configuration, and spatial short-range fading level) is examined. In particular, it is found that the received envelopes may be considered realizations of only locally stationary processes, even when movement in the propagation environment is homogeneous. The results presented may be used in the design of broad-band wireless LAN's and serve as a basis for the development of a theoretical model capable of predicting channel temporal variation characteristics under a variety of conditions.**

***Index Terms*—Indoor radio communication.**

I. Introduction

FUTURE broad-band wireless LAN's will have to operate in the millimeter wave bands in order to meet the requirements for higher data rates. For these systems, operating mainly in office buildings, the main source of channel temporal variations is often the movement of people in the vicinity of the stationary terminals. The characteristics of these human-induced variations can influence a number of design issues, such as the choice of the antennas, the multiple access and transceiver schemes, or the link budget. Therefore, it is required that they be accurately modeled under a variety of conditions.

Measurement and analysis of channel temporal variations is a challenging task, which has been attempted [1]–[7] for the UHF indoor channel, in most cases. The importance of the effects to characterize is likely to be strongly dependent not only on the degree and localization of movement, but also on many other parameters like the antenna heights and radiation patterns and the importance of multipath in the propagation environment. Moreover, as observed in [1], the temporal fading phenomenon is highly nonstationary. In the case of a millimeter wave channel, this nonstationarity characteristic will be shown to be present even if movement in the propagation environment is homogeneous. Because the number of possible traffic conditions and terminal configurations is so high, it is difficult to rely on channel simulators based strictly on empirical models to analyze the performance of a given system. Therefore, a theoretical ray-tracing model capable of predicting the statistics of temporal channel variations for specified propagation and human traffic conditions would be very useful. A prerequisite to the development of such a model is a thorough understanding of the mechanisms leading to the observed statistical behavior of the channel, for both narrow-band and wide-band cases.

The present work reports narrow-band experiments devoted to the study of the temporal fading phenomenon in a typical propagation environment near 30 GHz. In Section II, the propagation environment and measurement setup are described and the measurement procedure explained. Section III presents and analyzes results in terms of amplitude distributions, level crossing rates, average duration of fades, power spectrum density, and temporal correlations. Conclusions are presented in Section IV.

Manuscript received March 1, 1997; revised December 29, 1997. This work was supported by the Natural Science and Engineering Council of Canada (NSERC), the Fonds FCAR (Government of Quebec), Bell Canada, and INRS-Telecommunications.

P. Marinier is with Lucent Technologies, Holmdel, NJ 07733 USA.

G. Y. Delisle and C. L. Despins are with INRS-Telecommunications, Verdun, Québec, H3E 1H6 Canada.

Publisher Item Identifier S 0018-926X(98)04878-9.

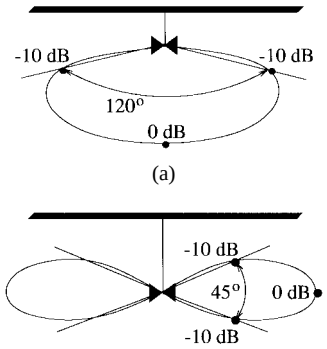

Fig. 1. Pattern shapes considered for the base antenna. (a) Type BS_1. (b) Type BS_2.

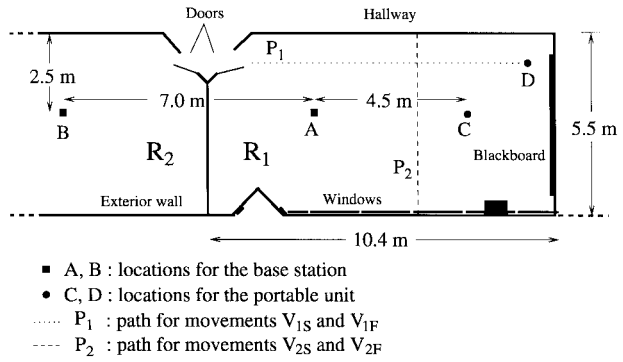

Fig. 2. Propagation environment.

II. Measurement Setup and Procedure

A. Propagation Scenario

Depending on the transmission losses through walls, which may range, according to the nature of the materials, from a

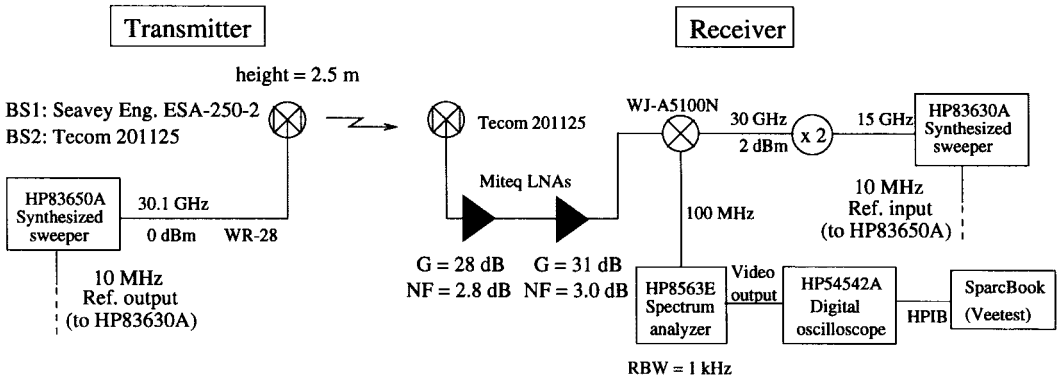

Fig. 3. Measurement setup.

few to several decibels near 30 GHz [8], a single base station may cover either a single room or a part of a story. This paper concentrates on the case where both terminals are located in a medium-sized room, the base station being positioned near the ceiling. Two kinds of pattern shapes are considered for the base antenna, as shown in Fig. 1. The first type (BS_1) points toward the floor with a weak directivity, while the second type (BS_2) is omnidirectional in the horizontal plane. For the portable unit, the simplest (and most likely) case is an omnidirectional pattern, which would not require aiming the unit toward the base station.

The propagation environment chosen for the measurements is depicted on Fig. 2. Most experiments took place in room R_1, although some have been carried out with the base station in room R_2. Plasterboard partitions separate the two rooms from each other and from the hallway. Relatively strong reflections could take place on windows (which are bordered by aluminum) and a blackboard. The floor is covered with a commercial rug and the height of the drop ceiling, which consists essentially of tiles and fluorescent lights, is 2.7 m. During the experiments, room R_1 was emptied to allow for free movements of walkers.

B. Measurement Setup

The measurement setup is outlined on Fig. 3. A CW signal at 30.1 GHz is transmitted by an antenna located at a height of 2.5 m ("base station"). Antenna type BS_1 is a linearly polarized scalar horn, whereas antenna type BS_2 is a linearly polarized biconical omnidirectional antenna. As illustrated on Fig. 1, the beamwidths of these antennas at 10 dB below the maximum intensity are, respectively, of 120° and 45°. An omnidirectional antenna of the same type as BS_2 is used at the receiving side ("portable unit"). After amplification, the received signal is downconverted to 100 MHz, then filtered and detected by a spectrum analyzer used in zero span mode. The resolution bandwidth (RBW) of the analyzer is set to 1 kHz, which is sufficiently wide to properly follow the fluctuations induced by Doppler effect on the waves reflected or diffracted by objects moving at speeds below 1.5 m/s (at 30.1 GHz). The video output of the analyzer is then sampled at 5 kHz by a digital oscilloscope connected via HPIB to a portable workstation for data recording. One acquisition consists in five shots of 32 768 samples totalizing about 32.8 s of record (the interval between consecutive shots is less than 0.5 s).

C. Terminal Configurations and Spatial Fading Level

Series of measurements were taken for six different terminal configurations (TC) specified by the chosen values of the following parameters: base location, base antenna type, portable unit location, and portable unit height h_p (Table I). The specification of these four parameters, however, is insufficient to ensure reproducibility of the results because of their observed strong dependence on the *spatial short-range fading situation* when the environment is free of movement. For given *macroscopic* locations of the antennas (i.e., specified to an accuracy of a few centimeters), it can be realized from a simple reasoning that the effects of movement may be radically different depending on whether the received envelope is in a fade or not when the environment is free of movement. This fading state is determined by the *fine* positions of the antennas relative to the fixed scatterers and, hence, is referred to as *spatial fading level* (R) in the following.

Assuming that the base station is fixed, R is a function of the fine position P_0 of the portable unit only and it can, therefore, be defined by

$$R(P_0) \equiv \frac{[\alpha(P_0)]^2}{L} \tag{1}$$

where $[\alpha(P_0)]^2$ is the received envelope power at P_0, and $L \equiv \overline{[\alpha(P)]^2}$ the *local spatial mean* of the received power for fine positions P of the portable unit in a region of a few square wavelengths around the specified macroscopic portable unit location. All these quantities are defined when the environment is free of movement so that the received envelope is constant over time for a given position of the portable unit. The local spatial mean L is a function of the terminal configuration only, whereas the spatial fading level R depends on the precise position of the portable unit in this configuration.

D. Measurement Procedure

In order to study the dependence of the temporal characteristics on R, it is necessary to estimate the local spatial mean L for each terminal configuration. Reasonably accurate estimates of this parameter have been obtained for each configuration by averaging the powers of 25 static measurements (room R_1 empty) taken for different fine positions of the portable unit around its specified macroscopic location. These 25 fine positions were separated from each other by at least one

TABLE I
TERMINAL CONFIGURATIONS

TC	Port. loc. (Fig. 2)	Base loc. (Fig. 2)	h_p (m)	Base ant. (Fig. 1)	Selected R values (dB)	Movements (Table II)
1	C	A	1.2	BS_1	5, 0, -5, 17	all
2	C	A	1.7	BS_1	3, -3, -7, -15	V, T
3	D	A	1.2	BS_1	2, -17	V, T
4	C	B	1.2	BS_1	4, -14	V, T
5	C	A	1.2	BS_2	5, -15	all
6	C	A	1.7	BS_2	7, -13	V, T

TABLE II
DESCRIPTION OF THE MOVEMENTS STUDIED

Mov.	Description
0	No movement (R_1 empty)
M_n	Random and uniform walk of n persons in R_1
V_{1S}	Walk along P_1 at $\sim$ 1.0 m/s
V_{2S}	Walk along P_2 at $\sim$ 0.9 m/s
V_{1F}	Walk along P_1 at $\sim$ 1.5 m/s
V_{2F}	Walk along P_2 at $\sim$ 1.3 m/s
T	Walk of one person along various selected trajectories (around the base, around the portable unit, etc.)

wavelength over an area of 5 $\lambda \times$ 5 λ ($\approx$25 cm^2), so as to obtain independent measurements. Then, for a given terminal configuration, a particular fine position of the portable unit is selected and the corresponding value for R is obtained by measuring the received envelope when the environment is free of movement, and dividing its power by L. Next, a set of measurements is taken while one or more persons are moving in R_1 according to different types of *movements* listed in Table II (movements V and T imply one person only). The spatial fading level R is measured again after the set of measurements is completed. Even if extreme care is taken to avoid contact with antennas, the value of R may vary *slowly* over a few decibels during the course of a set of measurements and this is believed to be the consequence of uncontrollable phenomena (like sudden displacements of windows due to wind). It has been checked that movement outside R_1 has no significant effect on the received envelope, except when the transmitter is located in R_2 in which case movement inside R_2 has also an influence.

For each terminal configuration, the set of measurements were taken for different approximate values of R ranging from -17 to 7 dB and indicated on Table I, along with the types of movements studied. Movements M_n have been studied for configurations one and five only. To ensure that the recording time of 32.8 s is sufficient to get statistically significant results, two acquisitions of 32.8 s have been taken and compared for each movement of configuration one. In the remaining portion of this paper, it is understood that the results for configuration one are for the combination of these two acquisitions (totalizing 65.5 s of recording).

III. RESULTS

Only typical results will be presented here, even if they are available for the different terminal configurations and types of movement. Differences obtained between the various configurations and types of movement will be pointed out if significant.

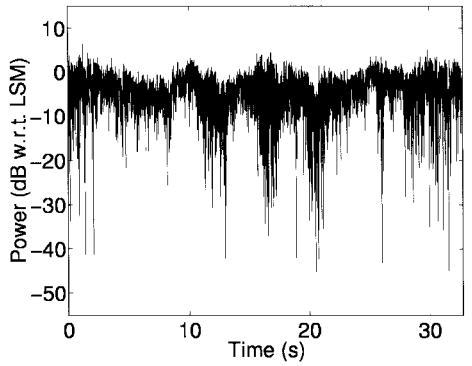

(a)

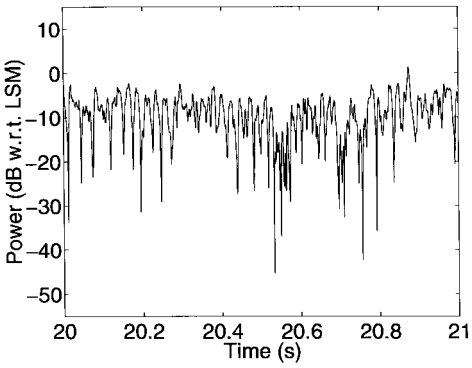

(b)

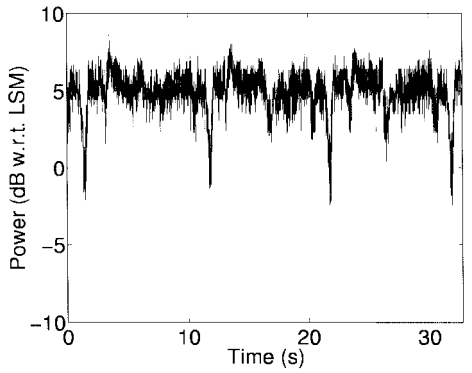

(c)

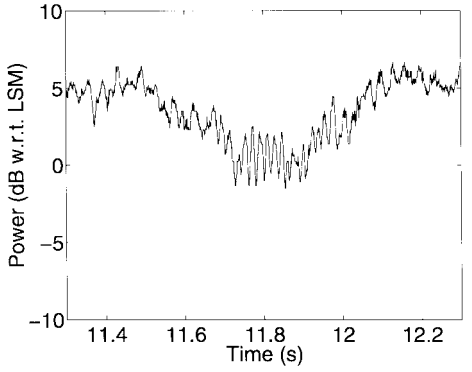

(d)

Fig. 4. Examples of measured envelopes. (a) TC 1, $R = -5$ dB, movement M_2. (b) Detail of fading over 1 s for the envelope shown in (a). (c) TC 1, $R = 5$ dB, movement T. (d) Detail of fading over one second for the envelope shown in (c).

TABLE III
ENVELOPE MEAN POWERS FOR TC 1 MOVEMENTS M_{1-4}

R (dB) Approx.	Movements 0	M_1	M_2	M_3	M_4
5	5.3/5.5	5.4	4.7	4.6	4.7
0	-0.4/0.5	0.8	0.6	0.7	0.3
-5	-5.9/-4.6	-3.5	-2.8	-2.9	-3.1
-15	-15.0/-14.5	-10.1	-7.2	-6.9	-6.1

TABLE IV
ENVELOPE STANDARD DEVIATIONS FOR TC 1 MOVEMENTS M_{1-4}

R (dB) Approx.	Movements 0	M_1	M_2	M_3	M_4
5	0.02/0.02	0.10	0.14	0.18	0.21
0	0.04/0.03	0.15	0.23	0.26	0.31
-5	0.02/0.04	0.25	0.35	0.37	0.41
-15	0.04/0.04	0.47	0.47	0.46	0.48

A. General Observations

Some examples of measured envelopes are shown on Fig. 4. Fig. 4(a) shows an envelope recorded while two persons were moving randomly in room R_1 (movement M_2) for TC 1, $R = -5$ dB. Fig. 4(b) shows the detail of fading over one second for this same envelope. From these two graphs it is apparent that the envelope is subject to very fast fluctuations superimposed on slower variations. Therefore, these envelopes should not be considered stationary processes over the duration of a complete acquisition (32.8 s), but only for a duration of about a few tenths of a second. In that case, such processes may be classified as *locally* (or quasi-) stationary. Fig. 4(c) shows an envelope recorded while one person was moving along a circle around the portable unit (movement T) for TC 1, $R = 5$ dB. Deeper fades appear periodically as the person obstructs the line-of-sight (LOS) path in passing between the base and the portable unit. The detail of the envelope over a period of time corresponding to one of these obstructions is shown on Fig. 4(d). It is clear that the quasi-stationary character of the envelope is also present in this case, despite the fact that the movement is perfectly regular and continuous.

B. Amplitude Distributions

The time-averaged mean power P and normalized standard deviation σ have been computed for each measured envelope according to the following formulas

$$P = \overline{\alpha^2(t)} \tag{2}$$

$$\sigma = \sqrt{\frac{\overline{[\alpha(t) - \overline{\alpha(t)}]^2}}{P}} \tag{3}$$

where $\alpha(t)$ is the linear envelope amplitude and the averages are taken over all data points of the recording. Even though it is likely from the preceding observations that the amplitude distribution may not be constant over time, the study of these parameters provides a good indication of the effect of movement on the amplitude properties of the envelope. In the following, the mean power is expressed in decibels relative to the local spatial mean L for the terminal configuration considered.

Tables III and IV show the values of P and σ of the measured envelopes for TC 1 movements M_{1-4}. The two values indicated for movement "0" (room R_1 empty) correspond to measurements taken at two different times to assess the stability of the spatial fading level.

From Table III it can be observed that the effects of movement on the mean power differ strikingly between the different R values. When the receiving antenna is on a spatial crest ($R \approx 5$ dB), the movement of people has little effect on the mean signal level. On the other hand, in the spatial-fade situation ($R \approx -15$ dB) the effect is a significant relative increase. The standard deviations (Table IV) are also sensitive to spatial fading, increasing systematically as R decreases from 5 dB to -15 dB. This behavior was to be expected: when the antennas are in a spatial-fade situation, this means that the stronger multipath components are adding in antiphase. When moving scatterers are introduced in the propagation environment, they obstruct one of more of these paths which are replaced by diffracted paths, whose phases and amplitudes are obviously different. This breaks the antiphase condition and results in a net increase of signal amplitude. For the opposite case, when the multipath components are adding in phase before the introduction of obstacles, the obstructions result in a decrease of signal amplitude. Similar reasoning can explain the behavior of standard deviations: when the signal level is very low, the disturbances caused by movement of persons have a much stronger effect than when the level is high. As the number of persons moving in the environment increases, it is apparent from Tables III and IV that the mean powers and standard deviations obtained for different R values tend to get closer. To confirm this trend, measurements have been done with about twenty persons walking randomly in the room (movement M_{20}) for TC 1 and two values of R (not exactly the same as those for movements M_{1-4} because practical constraints prevented a precise adjustment of R for these measurements). From the results of Table V, it can be noticed that the effect of the introduction of 20 persons has been to reduce the difference between the mean powers for the two values of R from 6.8 dB ($= 4.2 + 2.6$ dB) to 0.9 dB. The following intuitive explanation may help to understand the phenomenon: when the room is empty, the fading situation for given positions of the antennas is essentially determined by fixed or quasi-fixed scattering structures (walls, furnishing, etc.). As the number of moving scatterers is increased, the relative importance of the fixed scatterers tends to diminish, eventually vanishing in the limiting case when the room is crowded. At this point, the envelope properties are almost indifferent to the fine position of the antennas relative to the fixed scatterers.

The dependence of results on R in terms of mean power and standard deviations is observed for all other measurements. However, some differences of degree between the different configurations and types of movement have been noticed. For example, the effects on the mean power (increase or decrease) are much more accentuated when the direct path is blocked than for the other types of movements, which is in agreement

TABLE V
ENVELOPE MEAN POWER AND STANDARD DEVIATIONS FOR TC 1 MOVEMENT M_{20}

R (dB) approx.	Movements			
	0	M_{20}	0	M_{20}
	Mean Power		Standard Deviation	
4.2	4.2	0.7	0.02	0.39
−2.6	−2.6	−0.2	0.03	0.45

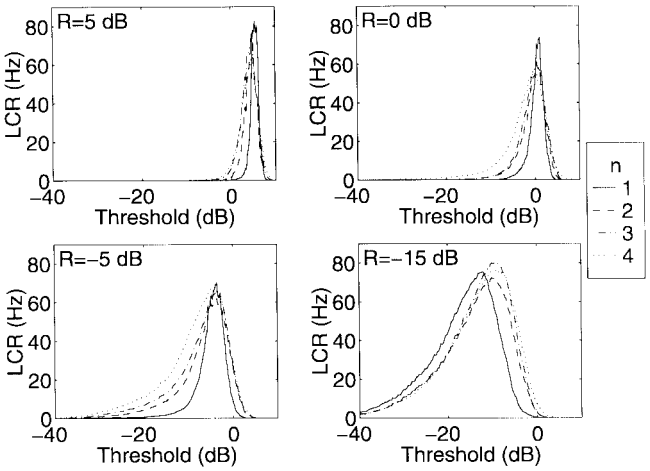

Fig. 5. LCR's for TC 1 movements M_{1-4}.

with the previous interpretation considering that the direct path is generally one of the strongest paths. Also, it has been observed that the effects of walking around the base are more accentuated than those of walking around the portable unit when the base antenna pattern type is BS_1 (TC 1, 2, 3, 4) and less accentuated when the base antenna type is BS_2 (TC 5, 6). The importance of the effect of a change of height for the portable unit is also dependent on the base antenna pattern: the variations are more reduced when the height of the portable unit is increased for pattern BS_2 (TC 5 and 6) than for pattern BS_1 (TC 1 and 2). These opposite trends can be easily explained after looking at the shapes of the two patterns on Fig. 1.

C. Level Crossing Rates and Average Fade Durations

The level crossing rate (LCR) at any specified threshold is defined as the rate at which the envelope crosses that threshold with a positive slope. The average period of a fade below that threshold is defined as the average fade duration (AFD) [9]. LCR's and AFD's have been computed for all measured envelopes and thresholds ranging from −40 dB to 10 dB. As for the mean powers, the thresholds are relative to the value of L for each terminal configuration (*not* to the root mean square (rms) values of each envelope) in order to obtain a fair comparison between the different R values. Results are shown on Figs. 5 and 6 for movements M_{1-4} and TC 1.

Comparison between the results of Fig. 5 and those shown on Tables III and IV indicates that the broadening and shift observed for the LCR curves, as the number of persons is increased, are closely related to the behavior of the mean power and the amplitude standard deviation. The maximum crossing rates observed on Fig. 5 are between 60 Hz and 85

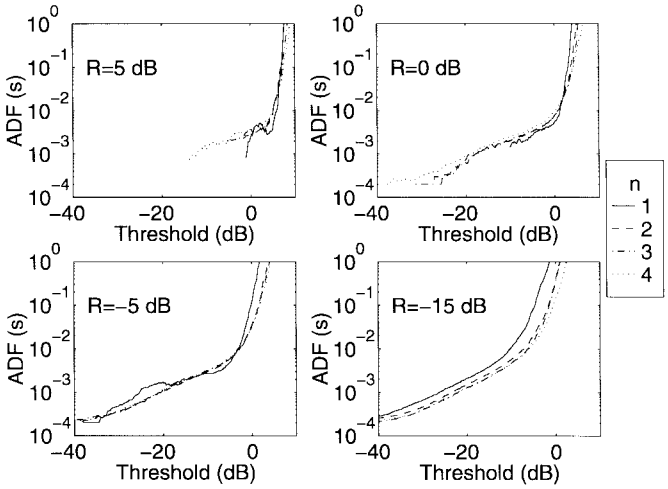

Fig. 6. AFD's for TC 1 movements M_{1-4}.

Hz, which corresponds roughly to the maximum crossing rates that would be experienced by the envelope received from a mobile terminal moving at a speed of 0.8 m/s with respect to the fixed terminal at 30 GHz under Rayleigh fading conditions [9]. These fast fluctuations are to be attributed to reflection/diffraction phenomena (onto/by the moving bodies), and this leads to the following interpretation for the mechanisms responsible for slow and fast envelope fluctuations: in the presence of moving obstacles in a multipath environment, the ray contributions may be categorized as "fixed" or "mobile" contributions. The fixed contributions are those associated to the direct path and those corresponding to reflections from fixed objects (such as walls) only. As obstacles move in the propagation environment in obstructing some of these paths, they engender variations whose coherence time is related to the speeds, sizes, and number of obstacles, but *not* to the wavelength. The mobile contributions are those associated to paths corresponding to reflections onto the moving bodies and diffraction by them. These contributions are subject to the Doppler effect as the corresponding path lengths change with the positions of bodies, thus, engendering variations whose coherence time is related to the speeds of bodies and to the wavelength. These variations are faster than the ones created by the obstructions because the human body is electrically large at millimeter wave frequencies. This explains the quasi-stationary behavior of the envelopes observed from inspection of measurements.

D. Power Spectrum Density

Since the envelopes are not stationary processes, their power spectrum densities (PSD) vary over time and a complete statistical characterization would, therefore, imply computing many PSD estimates for each envelope. An estimate of the *time-averaged* PSD for each envelope can be computed by using nonparametric methods, such as the method of Welch [10], which divides the data in windows. Fig. 7 shows the estimates of the time-averaged PSD for movements M_{1-4} and TC 1, computed using the method of Welch with Hanning windows of 102.4 ms duration (512 samples). This window

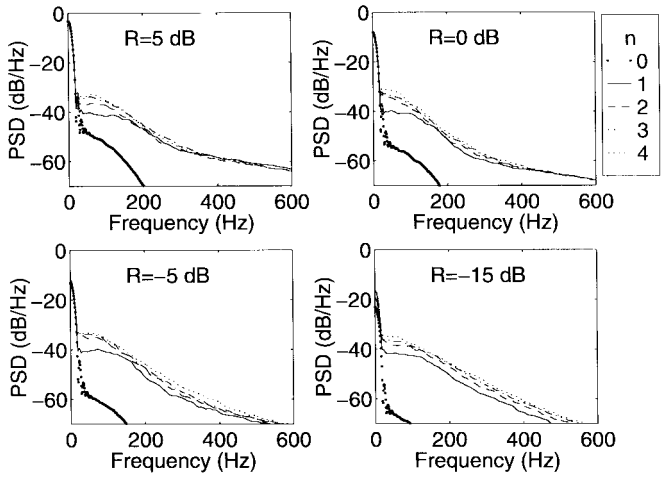

Fig. 7. PSD estimates for TC 1 movements M_{1-4}.

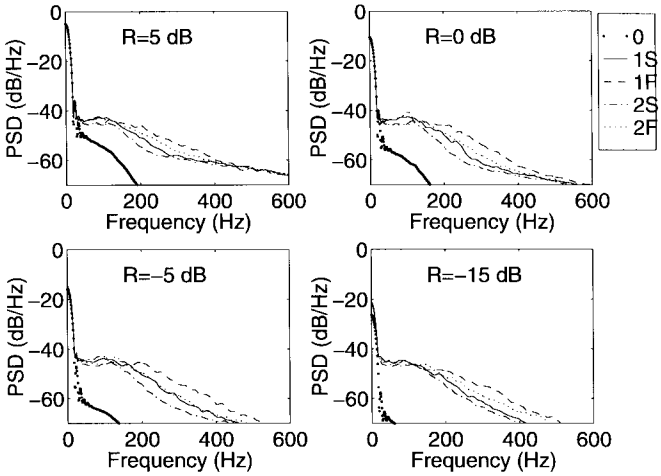

Fig. 8. PSD estimates for TC 1 movements V.

length has been chosen because it corresponds to a duration over which the envelopes can reasonably be considered locally stationary and it also gives a good compromise between frequency resolution and variance of the estimate.

On Fig. 7, the powers are still in decibels relative to the value of L for TC 1. It can be observed that the amplitudes of the sharp peak near 0 Hz are dependent on R, but not very significantly (at least on a logarithmic scale) on the number of walkers except for the deep-fade case ($R \approx -15$ dB). This is the opposite of the behavior of the PSD between dc and 150 Hz, which increases with the number of walkers, but is relatively insensitive to R. Fig. 7 shows also that the relative increase of energy (between dc and 100 Hz) with the number of walkers tends to be very small after two walkers.

Fig. 8 shows the estimates of the time-averaged PSD (computed using the same method) for movements V, TC 1. As it could be expected, the effect of increasing the speed of the walker is to widen the spectrum. Also, this figure shows that spectra widths for movements V_{1S} (along path P_1 at 1.0 m/s) and V_{2F} (along path P_2 at 1.3 m/s) are comparable. This implies that for the same speed, movement parallel to the direct path results in a broader spectrum than movement perpendicular. Results for other terminal configurations are similar.

E. Temporal Correlation

The correlation coefficient $\rho(\Delta t)$ between amplitudes separated by delay Δt may normally be computed when the envelope amplitude $\alpha(t)$ is a realization of a stationary process according to [7]

$$\rho(\Delta t) = \frac{\overline{(\alpha(t) - \overline{\alpha(t)})(\alpha(t+\Delta t) - \overline{\alpha(t+\Delta t)})}}{\sqrt{\overline{(\alpha(t) - \overline{\alpha(t)})^2}}\sqrt{\overline{(\alpha(t+\Delta t) - \overline{\alpha(t+\Delta t)})^2}}} \quad (4)$$

where averages are taken on all the data points of the recording. However, when $\alpha(t)$ is a realization of a process only locally stationary, the direct application of (4) results in an overestimation of ρ for Δt greater than a certain value owing to the differences between global and local averages. To overcome this problem, data from a single envelope were

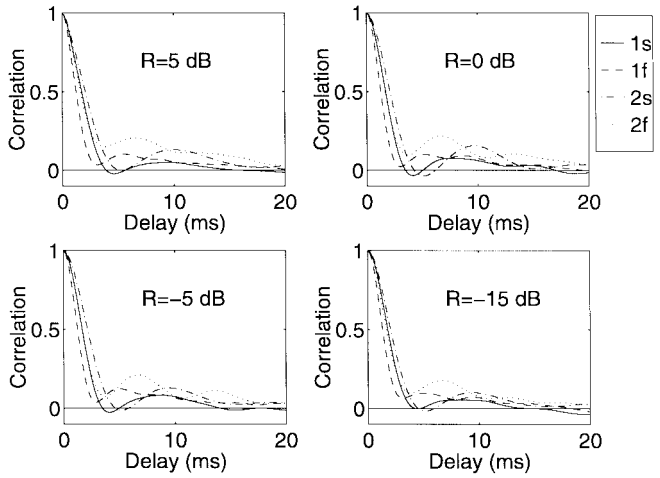

Fig. 9. Correlation coefficient estimates for movements V, TC 1.

first splitted in (rectangular) windows of 102.4 ms. Then the correlation coefficients were estimated for each window using (4) and a *time-averaged* correlation coefficient (similar to the time-averaged PSD) was defined as the average between results obtained from each window.

Fig. 9 shows the correlation coefficients for time differences (delays) up to 20 ms for movements V of TC 1, for which the speed of a single walker was controlled.

As expected, the widths of correlation curves for each movement follow the order inverse to that of spectra widths. Practically no dependence of the results on R can be observed for this characteristic. The time difference after which the correlation falls below 0.5 ("coherence time") is not greater than 3 ms for all speeds and trajectories. This remains true for the results of the other (not shown) configurations. However, correlation may fall more or less slowly beyond that delay depending on the specific configuration. For all configurations and types of movements, the coherence time has been found to lie between 0.1 and 0.3 times the ratio between the wavelength and the speed of the walker. It should be mentioned also that the precise values obtained may vary slightly depending on the window length chosen. Selection of a longer window results in a broadening of correlation curves.

IV. Conclusion

This paper reported measurements conducted near 30 GHz to study the effect of the movement of persons in the propagation environment on the temporal fading envelope for an indoor channel in which the two antennas are fixed during operation. The main results of this work may be summarized as follows.

1) When relatively few people (one to four) are moving in the multipath propagation environment, the main features of the amplitude distribution are strongly dependent on the spatial short-range fading state when the environment is free of movement. This dependence tends to become of lesser importance as the density of people increases.
2) In general, the envelopes may be considered as realizations of only locally stationary processes even when the movement of bodies in the environment is regular and continuous. This nonstationarity characteristic stems from the fact that human bodies become electrically "large" as the frequencies increase to millimeter wave bands.
3) Level crossing rates and average fade durations are also strongly dependent on the spatial fading level. The ranges of values obtained for these parameters are similar to what would be obtained for a mobile terminal moving approximately at the same speed as the walker(s).
4) For walking speeds between 0.9 m/s and 1.5 m/s at 30 GHz, the coherence time (for a correlation of 50%) is not greater than 3 ms.

This work will serve as a basis for the creation of a theoretical model for the prediction of the statistical behavior of an indoor millimeter wave channel under specified terminal configurations and human traffic conditions. The analysis shows that the inclusion of reflection/diffraction mechanisms is important to reproduce the quasi-stationarity character of the channel. Further experimental work is necessary to assess the importance of fluctuations on wide-band characteristics and is currently underway.

References

[1] R. J. C. Bultitude, "Measurement, characterization, and modeling of indoor 800/900 MHz radio channels for digital communications," *IEEE Commun. Mag.*, vol. 25, pp. 5–12, June 1987.

[2] T. S. Rappaport and C. D. McGillem, "UHF fading in factories," *IEEE J. Select. Areas Commun.*, vol. 7, pp. 40–48, Jan. 1989.

[3] R. J. C. Bultitude, S. A. Mahmoud, and W. A. Sullivan, "A comparison of indoor radio propagation characteristics at 910 MHz and 1.75 GHz," *IEEE J. Select. Areas Commun.*, vol. 7, pp. 20–30, Jan. 1989.

[4] S. J. Howard and K. Pahlavan, "Doppler spread measurements of indoor radio channels," *Electron. Lett.*, vol. 26, pp. 107–108, Jan. 1990.

[5] R. Ganesh and K. Pahlavan, "Statistics of short time variations of indoor radio propagation," in *Proc. Int. Conf. Commun.*, Denver, CO., June 1991, pp. 1.1.1–1.1.5.

[6] I. Oppermann, J. Graham, and B. S. Vucetic, "Modeling and simulation of an indoor radio channel at 20 GHz," in *Proc. Globecom*, Singapore, Nov. 1995, pp. 744–748.

[7] H. Hashemi, M. McGuire, T. Vlasschaert, and D. Tholl, "Measurements and modeling of temporal variations of the indoor radio propagation channel," *IEEE Trans. Veh. Technol.*, vol. 43, pp. 733–737, Aug. 1994.

[8] T. S. Rappaport, *Wireless Communications*, New York: IEEE Press, 1996.

[9] D. Parsons, *The Mobile Radio Propagation Channel*. New York: Wiley, 1992.

[10] J. G. Proakis and D. G. Manolakis, *Digital Signal Processing: Principles, Algorithms and Applications*, 2nd ed. New York: Macmillan, 1992.

Paul Marinier was born in Montreal, Québec, Canada, in 1971. He received the B.Sc. degree in physics from the University of Sherbrooke, Québec, Canada, in 1992, the M.Sc. and Ph.D. degree in telecommunications from INRS-Telecommunications, Verdun, Québec, Canada, in 1994 and 1998, respectively, and the Diplôme d'études Supérieures in piano from the Conservatory of Music of Rimouski, Québec, Canada.

He is now a member of technical staff at Lucent Technologies, Holmdel, NJ. His current research interests are in propagation modeling, digital communications, and wireless communications.

Gilles Y. Delisle (S'63–M'73–SM'86) was born in Quebec City in 1945. He received the Ph.D. degree from Laval University, Quebec, Canada, in 1973.

He has been a Professor of Electrical Engineering at Laval University, Quebec, Canada, since 1973, where he was head of the Department from 1977 to 1983. From June 1992 to June 1997, he was also Director of INRS Telecommunications, a research institute which is a part of the Université du Québec. He has been a consultant in many countries He is involved in research work in radar cross-section measurements and analytical predictions, mobile radio-channel propagation modeling, personal communications, and industrial realization of telecommunications equipment.

Dr. Delisle is a senior member of the Order of Engineers of the Province of Quebec, President of the Canadian Engineering Accreditation Board, a member of URSI (Commission B and C) ACFAS, and a Fellow of the Engineering Institute of Canada. His work in technology transfer has been recognized by a Canada Award of Excellence in 1986. In 1986 he was awarded the J. Armand Bombardier prize of ACFAS (Association Canadienne Française pour l'Avancement des Sciences) for outstanding technical innovation.

Charles L. Despins received the B.Eng. degree in electrical engineering from McGill University, Montréal, PQ, Canada, in 1984, and the M.Eng. and Ph.D. degrees from Carleton University, Ottawa, ON, Canada, in 1987 and 1991, respectively.

From 1984 to 1985, he was with CAE Electronics, Montréal, PQ, Canada, as a member of the technical staff working on the design of flight simulators. During 1991 to 1992 he was with the Department of Electrical and Computer Engineering of École Polytechnique de Montréal as a lecturer and research engineer under the auspices of the Canadian Institute for Telecommunications Research (CITR), Montréal. Since 1992 he has been on the faculty of INRS-Télécommunications (Université du Québec), Montréal, where he is currently an Associate Professor of electrical engineering and where he has previously served as a consultant to various telecommunication operators and manufacturers. Since 1996 he has also been with Microcell Connexions Inc. (Canadian GSM operator), Montreal, PQ, Canada, where he is currently Director of Research & Standards and responsible for radio access and network infrastructure R&D as well as standards issues. His research and technical interests are in signal processing for digital communications with emphasis on mobile and portable radio systems.

Dr. Despins was awarded the IEEE Vehicular Technology Society Best Paper of the Year Prize in 1993. He is a member of the Order of Engineers of Québec.